



Ribose Found in the Gas Phase**

Emilio J. Cocinero,* Alberto Lesarri,* Patricia Écija, Francisco J. Basterretxea, Jens-Uwe Grabow, José A. Fernández, and Fernando Castaño

Sugars are clearly of biochemical interest as cellular energy fuels, metabolic intermediates, mediators of cellular interactions, or structural building blocks. Recently the interest in sugars has been boosted by the quest for organic molecules in interstellar space.^[1] The detection of prebiotic building blocks is relevant both to cosmochemistry and biology, since it could trace the construction of molecular complexity and provide a competing mechanism for the emergence of life on Earth. Simple C₂^[2] and C₃^[3] sugar building blocks have been found in molecular clouds and meteorites. However, the search for more complex sugars is hampered by a serious lack of accurate structural and spectroscopic information. Sugars are small molecules but structurally complex and elusive to experimental methods: the C₅ D-aldose sugar, ribose, was only elucidated by X-ray crystal diffraction in 2010.^[4] At that time it was stated that ribose was “recalcitrant to crystallization”, requiring advanced zone-melting recrystallization techniques and complementary ¹³C MAS NMR data.^[4] Even when diffraction methods are feasible, their structural description is biased by crystal packing forces and it may not reflect the most stable structure for the isolated molecules.^[5] NMR spectroscopic methods conducted in condensed phases offer solvent-averaged indirect structures^[6] and do not represent an independent solution either.

These difficulties are notorious for sugars since they are polymorphic systems. According to any standard textbook aldopentoses, such as ribose, can exhibit either linear forms or cyclic five-membered (furanose, fur) or six-membered (pyranose, pyr) rings, occurring either as α or β anomers depending on the orientation of the hydroxy group at C1 in Scheme 1 (anomeric carbon). Ribose is usually depicted as a β -furanose, predominant in ribonucleosides, RNA, ATP, and other biochemically relevant derivatives. Probably for this reason a computational study surprisingly considered only the β -furanose form.^[7] However, early NMR spectroscopy experiments suggested that the dominant form of ribose in aqueous solution was not β -furanose but β -pyranose, with the four ring species coexisting with ratios β -pyr: α -pyr: β -fur: α -fur = 62:20.3:11.6:6.1.^[6] In the 2010 X-ray/NMR study the crystal was reported to be composed of pyranoses with a β : α ratio of 1.7–2:1, but stating that “it is difficult to estimate the reliability of these ratios” because of the different sample conditions. Furanose and pyranose rings exhibit additional conformational variations, making the system more difficult. Pyranoses have a relatively rigid chair skeleton^[8] with dominant conformations ¹C₄ or ⁴C₁ (see Scheme 1) connected by ring inversion (⁴C₁-chair rings were reported in the X-Ray/NMR study^[4]). Plausible boat structures might be also considered in ribopyranoses, although probably less favored. On the other hand furanoses are more flexible,^[9] because of the possibility of interconverting different envelope forms such as C₂-endo or C₃-endo through non-planar structures (“pseudorotation”^[10]). The multiple hydroxy groups finally add conformational complexity since each hydroxy group may produce many rotamers. The conflicting conformational ratios from the X-ray and NMR studies suggest that all these simultaneous effects are difficult to disentangle in condensed phases and give rise to several questions. Is the RNA-analogue β -fur representative of free ribose? What is the relative stability of α and β anomers? Can linear forms of sugars be observed in the isolated molecule? Finally, what are the preferred conformations of ribose: furanoses, pyranoses, or linear chains?

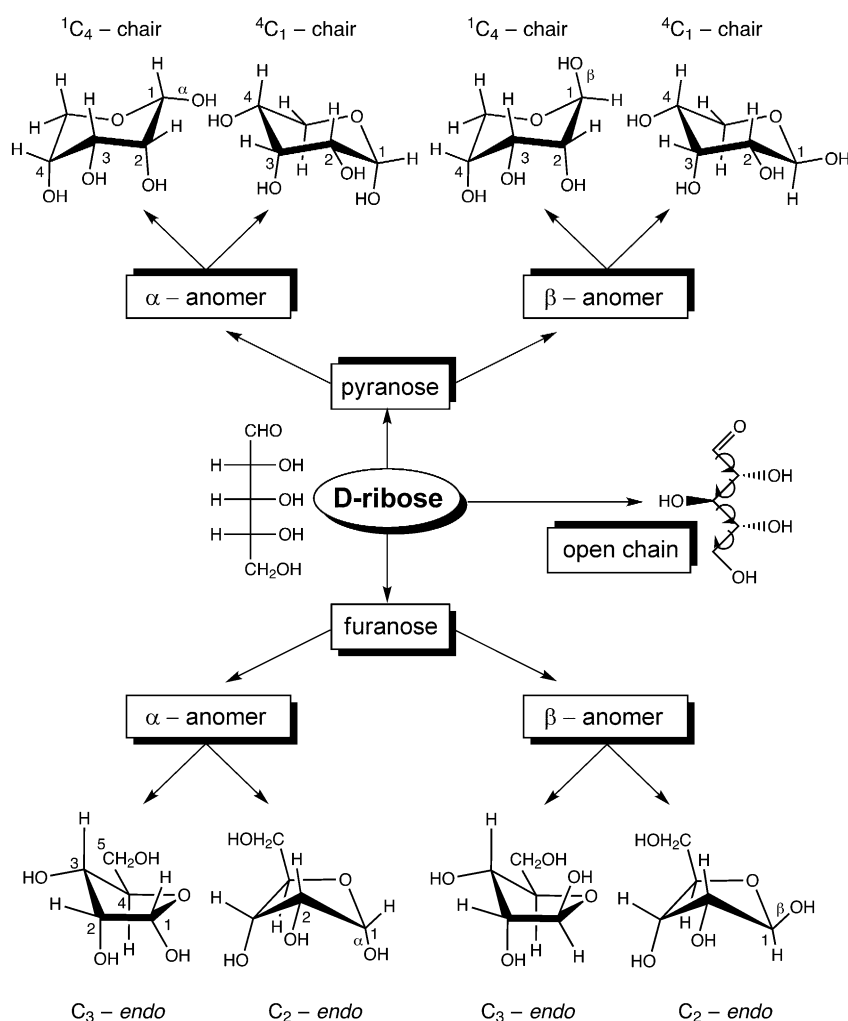
To answer these questions we conducted a rotational study of ribose using microwave spectroscopy. A large volume of structural information on chromophore-tagged sugars has been collected by the Simons' group^[11–13] using UV–UV and IR–UV laser spectroscopy techniques and theoretical calculations.^[14] However, laser spectroscopy provides only vibrational resolution and band assignment is not always unambiguous. Conversely, pure rotational spectroscopy requires no chromophore, offers very high (sub-Doppler) resolution, and leads to accurate moments of inertia for the isolated molecule.^[15] Rotamers and isotopologues can thus be dis-

[*] Dr. E. J. Cocinero, Dr. P. Écija, Dr. F. J. Basterretxea, Dr. J. A. Fernández, Prof. F. Castaño
Departamento de Química Física, Facultad de Ciencia y Tecnología
Universidad del País Vasco (UPV-EHU)
Apartado 644, 48080 Bilbao (Spain)
E-mail: emiliojose.cocinero@ehu.es
Homepage: <http://www.grupodeespectroscopia.es/MW>
Prof. A. Lesarri
Departamento de Química Física y Química Inorgánica
Facultad de Ciencias, Universidad de Valladolid
47011 Valladolid (Spain)
E-mail: lesarri@qf.uva.es
Homepage: <http://www.uva.es/lesarri/>
Prof. J.-U. Grabow
Institut für Physikalische Chemie & Elektrochemie
Gottfried-Wilhelm-Leibniz Universität Hannover
Callinstrasse 3A, 30167 Hannover (Germany)

[**] Financial support from the Spanish Ministry of Science and Innovation (MICINN, 2010/CSD2007-00013, CTQ2009-14363, CTQ2011-22923), and the Basque Government (Consolidated Groups) is gratefully acknowledged. J.U.G. thanks additionally the Deutsche Forschungsgemeinschaft and the Land Niedersachsen. E.J.C. acknowledges also a “Ramón y Cajal” contract from the MICINN. Computational resources and laser facilities of the UPV-EHU were used in this work (SGIker and I2Basque).



Supporting information for this article is available on the WWW under <http://dx.doi.org/10.1002/anie.201107973>.



Scheme 1. Structural polymorphism in D-ribose.

cerned as independent species and the resulting structures can be used directly for radio-astronomical search and to benchmark the theoretical models.

Attempts to record the rotational spectra of sugars have, so far, proved unsuccessful. Ribose was investigated by Lovas and Motiyenko^[16] using heating methods, but thermal instability resulted in *cis*-/*trans*-furfural and other minor compounds.^[17] Later attempts by Grabow and Fritzsche^[18] used IR laser ablation, but resulted also in decomposition products.^[19] Herein we chose to combine microwave spectroscopy in supersonic jets with ultrafast UV laser vaporization, using our recently built FT-MW spectrometer in Bilbao.^[20] This approach was previously co-developed by us^[21] and proved successful both for bioorganic (i.e., amino acids^[21,22]) or metallic species.^[23]

The rotational study of ribose required an exhaustive conformational search. For this purpose multiple molecular structures belonging to the linear chain, α/β -fur and α/β -pyr structural classes were tentatively screened using a fast molecular mechanics method (MMFFs^[24]) and advanced Monte-Carlo and large-scale low-mode conformational search algorithms. After a satisfactory conformational

energy window (25 kJ mol^{-1}) was achieved, the 70 lowest lying conformations were re-optimized using both density-functional theory (DFT) and abinitio (MP2) methods. Two different DFT methods (B3LYP and M06-2X^[25]) were compared to ensure the internal consistency of the theoretical models and their predictive values. Additionally, the calculation of vibrational frequencies provided the harmonic force field required for the centrifugal distortion constants. Once a large repertoire of plausible structures was available we initiated the scan of the microwave spectrum. The initial survey scan in Figure 1 revealed a congested spectrum with a large number of rotational transitions, which disappeared when laser vaporization was turned off. Since ribose was not expected to exhibit fine (i.e., internal rotation) or hyperfine effects (i.e. nuclear quadrupole coupling) the rotational transitions did not show any recognizable internal features and the spectra were assigned searching for combinations of the characteristic patterns of the *R*-branch μ_a transitions,^[26] predicted to be active for the most stable conformers. After a multiple iterative process the spectral search finally rendered the rotational signatures of six separate species. The measured transitions, covering angular momentum quantum numbers $J = 3-6$, fitted very satisfactorily to a Watson semi-rigid rotor model^[27] (root mean square

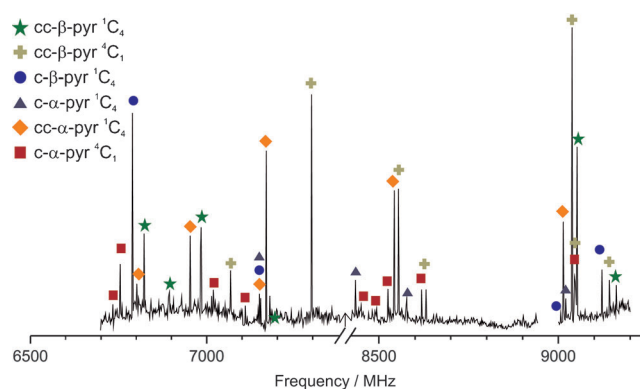


Figure 1. A section of the jet-cooled microwave spectrum of D-ribose.

(rms) deviation $< 2 \text{ kHz}$). Tunneling effects arising from the hydroxy groups were not noticeable. The experimental rotational constants and centrifugal distortion parameters are presented in Table 1. The frequencies of the rotational transitions are collected in the Supporting Information (Tables S1–S6). Following the spectral analysis some unas-

Table 1: Rotational parameters of the six observed conformations of D-ribose (A–F).

Parameter	Conformer A cc-β-pyr ¹ C ₄	Conformer B cc-β-pyr ⁴ C ₁	Conformer C c-β-pyr ¹ C ₄	Conformer D c-α-pyr ¹ C ₄	Conformer E cc-α-pyr ¹ C ₄	Conformer F c-α-pyr ⁴ C ₁
A ₀ [MHz] ^[a]	1844.98735 (18) ^[c]	2048.18674 (41)	1853.13790 (95)	1954.0129 (30)	1960.29176 (39)	1886.47378 (71)
B ₀ [MHz]	1305.135870 (74)	1176.32050 (22)	1301.195100 (89)	1267.42042 (25)	1272.44554 (21)	1280.03450 (25)
C ₀ [MHz]	1087.84195 (10)	845.23676 (21)	1081.87037(10)	1000.48929 (28)	994.58926 (20)	995.20684 (25)
A _e [MHz]	1851	2060	1863	1966	1967	1886
B _e [MHz]	1313	1179	1306	1270	1279	1288
C _e [MHz]	1094	849	1089	1006	999	1000
D _J [kHz]	0.0646 (15)	0.0246 (22)	0.0682 (14)	0.0465 (44)	0.0597 (19)	0.0342 (52)
D _{JK} [kHz]		0.110 (18)				0.215 (63)
d _J [Hz]		-7.4 (1.7)			-14.7 (1.7)	
μ _a [D]	1.4	2.0	1.7	2.9	2.1	1.2
μ _b [D]	0.9	0.1	0.2	1.3	0.5	2.0
μ _c [D]	1.0	1.2	0.7	1.7	1.3	1.2
N	29	27	20	14	24	18
σ [kHz]	1.0	1.5	0.8	2.0	1.4	2.0
				5	4	6
ΔG ^{EXP} [kJ mol ⁻¹] ^[b]	0.0	0.0(6)	2.1(7)	4.6(9)	1.6(3)	1.6(3)
ΔG ^{THEO} [kJ mol ⁻¹]	0.0	0.2	1.0	1.3	3.1	3.5

[a] Experimental ground-state (A₀, B₀, C₀) and predicted equilibrium (A_e, B_e, C_e) rotational constants, determinable centrifugal distortion constants (D_J, D_{JK}, d_J), electric dipole moment components (μ_a, μ_b, μ_c) from the MP2 calculations, number of fitted transitions (N) and MW rms deviation of the fit (σ). [b] Gibbs free energies estimated from the relative intensities of the microwave transitions (ΔG^{EXP}) and theoretical values calculated from the MP2 conformational search in Table 2 (ΔG^{THEO}). [c] Standard error in parentheses in units of the last digit.

signed lines remained in the spectrum, but they were not identified as ribose species.

To ascertain which ribose conformations were the carriers of the spectrum we compared the experimental rotational parameters of Table 1 with the theoretical predictions in Table 2 and Figure 2 (full rotational parameters in Supporting Information, Tables S13–S15). Several key points resulted from this comparison. The most stable conformation of ribose is a β-pyr ¹C₄ ring. The structural assignment is unequivocal from the small relative differences (< 0.6 %) in the rotational constants and is consistent with the line intensities and the predictions for the electric dipole moments. Using similar arguments the second and third most-stable conformers of D-ribose are also β-anomers. However, they differ in the ring configuration, adopting either a ⁴C₁ or ¹C₄-chair, respectively. Conversely, the three conformations predicted with the next higher energies are α-pyr. We observe in these cases a similar pattern of structural variations. Two of the observed conformations are ¹C₄ chairs, while the other conformer displays a ⁴C₁ ring (because of the similar structures the dipole moments were instrumental in this case). An estimation of the conformational energies obtained from relative intensities of the microwave transitions^[28] is presented in Figure 3 and Table 1. This calculation works on the assumption that conformational relaxation is negligible and that molecular populations are effectively cooled down in the expansion to the vibrational ground-state of each conformational well. However, conformational relaxation cannot be totally excluded in this molecule, so these conformational energies are to be considered only tentatively. Despite these cautions, the agreement between our observations and the theory is

Table 2: Conformational search of D-ribose below 10 kJ mol⁻¹ (all pyranoses), together with the most stable α- and β-furanoses and the lowest lying linear form (see Figure 2 for an extended plot).

Conformer	Conformation	Experiment	MP2 ^[a] ΔE (ΔG)	M06-2X ΔE (ΔG)	B3LYP ΔE (ΔG)
1	β-pyr ¹ C ₄	A	0.0(0.0)	0.0(0.0)	0.5(1.4)
2	β-pyr ⁴ C ₁	B	1.2(0.2)	2.8(2.1)	0.0(0.0)
3	β-pyr ¹ C ₄	C	1.2(1.0)	1.0(0.9)	1.4(2.2)
4	α-pyr ¹ C ₄	D	1.5(1.3)	1.6(1.6)	1.8(2.7)
5	α-pyr ¹ C ₄	E	2.8(3.1)	3.2(3.6)	3.0(4.2)
6	α-pyr ¹ C ₄		3.4(3.3)	2.1(2.0)	3.2(3.9)
7	α-pyr ⁴ C ₁	F	3.4(3.5)	2.4(2.6)	2.2(3.3)
8	β-pyr ¹ C ₄		4.9(4.3)	4.8(4.3)	5.6(6.1)
9	β-pyr ¹ C ₄		6.3(4.9)	6.8(6.4)	6.8(6.9)
10	α-pyr ¹ C ₄		6.3(6.1)	6.5(6.3)	6.0(6.7)
11	α-pyr ⁴ C ₁		8.0(7.6)	7.5(7.3)	7.5(8.0)
12	α-pyr ⁴ C ₁		8.2(8.0)	6.8(6.7)	6.7(7.6)
13	α-pyr ⁴ C ₁		9.2(8.3)	9.9(10.0)	8.5(8.9)
15	α-fur		11.8(9.1)	14.8(12.1)	9.0(6.7)
19	β-fur		15.8(11.3)	22.1(17.6)	12.4(8.0)
31	linear		18.7(13.1)	27.4(22.1)	4.8(0.3)

[a] Electronic energies including zero-point energy correction (ΔE, kJ mol⁻¹) and Gibbs free energies (ΔG at 298 K and 1 atm, kJ mol⁻¹, in parentheses) using MP2, M06-2X, and B3LYP methods.

generally satisfactory. Both α- and β-pyr were predicted to be more stable than furanoses (MP2: ΔG₂₉₈ ≥ 9 kJ mol⁻¹) or the linear form (MP2: ΔG₂₉₈ ≥ 13 kJ mol⁻¹). Moreover, the three most-stable structures predicted for ribose are β-anomers and slightly more stable than the other α-pyranoses (the relative intensities suggest a lower than predicted conformational

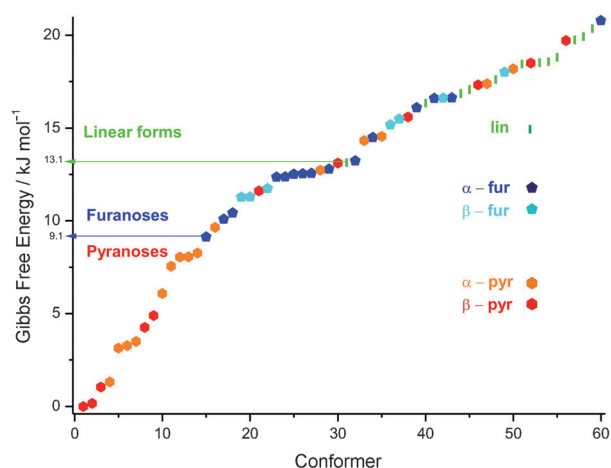


Figure 2. Predicted Gibbs free energies (MP2) for the 60 most-stable conformations of D-ribose.

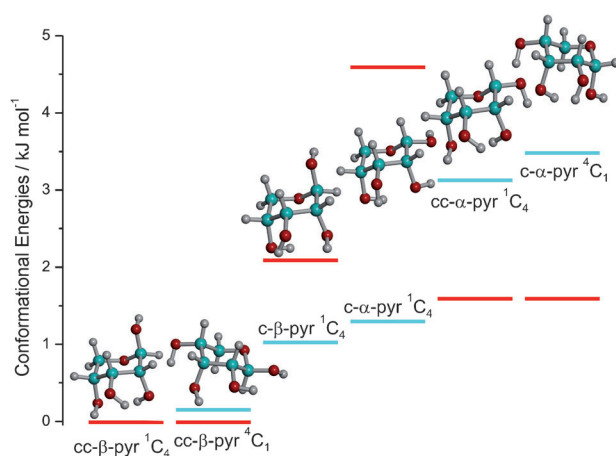


Figure 3. The six detected conformations of free ribose are six-membered pyranose rings, adopting 1C_4 - or 4C_1 -chair structures. The three predicted lowest-lying conformers are β anomers, the remaining three adopting the alternative α configuration. The conformational energies in red are estimations derived from the relative intensities of the microwave transitions. The blue horizontal lines represent the theoretical (MP2) ΔG_{298} predictions in Table 2.

energy of the last two conformers close to the third one). Globally, we observe six of the seven predicted lowest-lying conformations, spanning an energy window of 4.6(9) (MP2: 3.5) kJ mol^{-1} . The non-observation of conformer 6 in Table 2 can be safely attributed to a collisional relaxation in the jet,^[29] since it differs from conformer 5 only in the orientation of the hydroxy group at C1. Cooperative hydrogen bonding is noticeably in all the observed conformers, as previously discerned for other saccharides using vibrational spectra.^[11] In the 1C_4 global minimum the hydroxy groups in carbon atoms 2–4 orient themselves to adopt a network of three (across-ring and vicinal) intramolecular hydrogen bonds $\text{O2-H(axial, Ax)} \rightarrow \text{O4-H (Ax)} \rightarrow \text{O3-H (equatorial, Eq)}$ as in Figure 4 (full structure in Table S7). Using a conventional notation based on the Haworth projection this configuration is labeled as counter-clockwise (cc; viewed from above), so the most stable

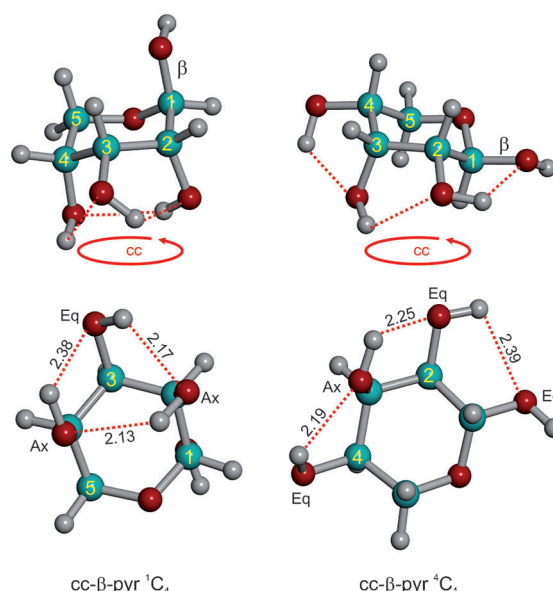


Figure 4. Cooperative intramolecular hydrogen-bond networks (dotted lines) involving the vicinal or across-ring hydroxy groups in the two most stable conformations of ribose $\text{cc-}\beta\text{-pyr } ^1C_4$ and $\text{cc-}\beta\text{-pyr } ^4C_1$ (distances in Å from the MP2 structure in Supporting Information, Tables S7–S8). Ring conformation and axial (Ax)/equatorial (Eq) hydroxy orientations result in three different ranges of hydrogen-bond lengths (see text). C blue (position number indicated), O red, H gray.

ribose structure would be $\text{cc-}\beta\text{-pyr } ^1C_4$. Because of the 1C_4 chair the hydroxy group at C1 (Ax) is relatively free and no intramolecular hydrogen bonding is possible, adopting a *trans* orientation respect to C2. The second most stable conformer is 4C_1 (O1-H Eq), so all four hydroxy groups can engage in a counter-clockwise series of intramolecular hydrogen bonds $\text{O4-H(Eq)} \rightarrow \text{O3-H(Ax)} \rightarrow \text{O2-H(Eq)} \rightarrow \text{O1-H(Eq)}$, denoted $\text{cc-}\beta\text{-pyr } ^4C_1$ (Figure 4 and Supporting Information, Table S8). The third predicted conformation has the same structure as the global minimum, but with the hydroxy groups in a reverse clockwise (c) direction, or $\text{c-}\beta\text{-pyr } ^1C_4$ (Supporting Information, Figure S1 and Table S9). The α -pyranoses display again both clockwise and counter-clockwise orientations, denoted respectively $\text{c-}\alpha\text{-pyr } ^1C_4$, $\text{cc-}\alpha\text{-pyr } ^1C_4$ and $\text{c-}\alpha\text{-pyr } ^4C_1$ (see Tables S10–12 and Figure S1 in the Supporting Information).

Several conclusions emerge from this work. We found no evidence of either α - β -furanoses or any linear forms in gaseous ribose, confirming that the free molecule adopts preferentially β -pyranose and higher-energy α -pyranose forms. The theoretical population ratio (MP2) $\beta\text{-pyr}:\alpha\text{-pyr}:\beta\text{-fur}:\alpha\text{-fur}:\text{linear} = 63.8:35.8:0.35:0.04:0.00$ and that of $\beta\text{-pyr}:\alpha\text{-pyr} = 65.4:32.5$ obtained from relative intensities are comparable but strikingly different from the values in solution,^[6] where despite the predominance of the pyranose structures, the furanoses have larger abundances than in the gas phase. The agreement between the conformational ratios obtained from relative intensities and the free energies suggests that ultrafast laser vaporization initially provides thermal equilibrium populations,^[30] which might be preserved in the expansion if collisional relaxation were negligible. The

global minimum, cc- β -pyr 1C_4 , and three other structures exhibit a 1C_4 -chair conformation, contrasting with the most stable 4C_1 -chairs observed in the α -/ β -aldo-hexoses and its deoxy derivatives detected with electronic spectroscopy: phenylglucose, phenylgalactose, phenylmannose, phenylfucose, and aldopentose phenylxylose.^[12] However the stabilization of the 1C_4 -chair is not large, since the second 4C_1 ribose conformation is practically isoenergetic with the global minimum ($\Delta G = 0.0(6)$ kJ mol⁻¹; MP2: $\Delta G = 0.2$ kJ mol⁻¹). The two chair conformations are associated with different (Ax/Eq) hydroxy orientations, which in turn, favor different intramolecular hydrogen bonds between vicinal or across-ring hydroxy groups. The number and strength of the available hydrogen-bond contacts is thus probably the primary factor determining conformational stability. Because of the geometry constraints of the tetrahydropyran chair the stronger hydrogen-bond contacts are between hydroxy groups in positions Ax–Ax (1.9–2.1 Å), and decrease for Ax–Eq or Eq–Ax (2.2–2.4 Å) and Eq–Eq (2.4–2.5 Å) orientations, as shown in Figure 4 and Supporting Information Figure S1. Similar hydrogen-bond patterns were observed in the hexoses and pentoses^[12] (although in these previous cases all O3-H groups were equatorial). While 4C_1 chairs have most of the hydroxy groups equatorial, the stability of 1C_4 chairs with all hydroxy groups axial raises additional questions on the magnitude of plausible stereoelectronic contributions, such as the anomeric effect,^[31,13] which would modulate conformational populations favoring β forms in 1C_4 and α forms in 4C_1 . As a consequence the conformational equilibrium may be determined ultimately by a subtle combination of ring conformation, intramolecular hydrogen bonds, and orbital interactions.

The results of this work may also have an impact on issues concerning the early evolution of biochemical building blocks containing ribose. Both the thermal instability and the observed preference for the pyranose rings in the free molecule seem to exclude the possibility that the first genetic material might have contained ribose, as previously suggested.^[17] Finally, our work emphasizes the importance of structural studies based on modern rotational techniques, which are still far from being fully exploited.

Experimental Section

The FT-MW spectrometer^[15,32] at the UPV-EHU has been described elsewhere.^[20] For this experiment the pulsed solenoid valve was attached to a Smalley-type^[33] laser desorption nozzle, as previously implemented.^[34,35,21] D-ribose (98 %) was pressed to form target rods and vaporized with a 355 nm picosecond Nd:YAG laser (ca. 5 mJ pulse⁻¹). Neon (3–6 bar) was used as carrier gas.

The quantum mechanical calculations used Gaussian 2009,^[36] running in two supercomputers (870 and 1400 processors) with a maximum of 96 processors per calculation. The theoretical methods included frozen-core MP2 perturbation theory, and Becke's (B3LYP) and Truhlar's dispersion-corrected M06-2X functional,^[25] with a standard 6-311++G(d,p) basis set.

Received: November 12, 2011

Published online: December 28, 2011

Keywords: conformational analysis · hydrogen bonding · ribose · rotational spectroscopy · sugars

- [1] a) E. Herbst, E. F. van Dishoeck, *Annu. Rev. Astron. Astrophys.* **2009**, *47*, 427; b) P. Ehrenfreund, J. Cami, *Cold Spring Harbor Perspect. Biol.* **2010**, *2*, a002097.
- [2] a) W. M. Irvine, R. D. Brown, D. M. Cragg, P. Friberg, P. D. Godfrey, N. Kaifu, H. E. Matthews, M. Ohishi, H. Suzuki, H. Takeo, *Astrophys. J.* **1988**, *335*, L89; b) J. M. Hollis, P. R. Jewell, F. J. Lovas, A. Remijan, H. Mollendal, *Astrophys. J.* **2004**, *610*, L21.
- [3] a) J. M. Hollis, F. J. Lovas, P. R. Jewell, *Astrophys. J.* **2000**, *540*, L107; b) J. M. Hollis, S. N. Vogel, L. E. Snyder, P. R. Jewell, F. J. Lovas, *Astrophys. J.* **2001**, *554*, L81; c) J. M. Hollis, P. R. Jewell, F. Lovas, P. Remijan, *Astrophys. J.* **2004**, *613*, L45; d) D. T. Halfen, A. J. Apponi, N. Woolf, R. Polt, L. M. Ziurys, *Astrophys. J.* **2006**, *639*, 237.
- [4] a) D. Šišak, L. B. McCusker, G. Zandomenighi, B. H. Meier, D. Bläser, R. Boese, W. B. Schweizer, R. Glymour, J. D. Dunitz, *Angew. Chem.* **2010**, *122*, 4605; *Angew. Chem. Int. Ed.* **2010**, *49*, 4503; b) W. Saenger, *Angew. Chem.* **2010**, *122*, 6633; *Angew. Chem. Int. Ed.* **2010**, *49*, 6487.
- [5] a) E. J. Cocinero, A. Lesarri, P. Écija, J.-U. Grabow, J. A. Fernández, F. Castaño, *Phys. Chem. Chem. Phys.* **2010**, *12*, 6076; b) A. Lesarri, E. J. Cocinero, L. Evangelisti, R. D. Suenram, W. Caminati, J.-U. Grabow, *Chem. Eur. J.* **2010**, *16*, 10214.
- [6] a) M. Rudrum, D. F. Shaw, *J. Chem. Soc.* **1965**, 52; b) R. U. Lemieux, J. D. Stevens, *Can. J. Chem.* **1966**, *44*, 249; c) E. Breitmaier, U. Hollstein, *Org. Magn. Reson.* **1976**, *8*, 573.
- [7] A. F. Jalbout, L. Adamowicz, L. M. Ziurys, *Chem. Phys.* **2006**, *328*, 1.
- [8] E. L. Eliel, S. H. Wilen, *Stereochemistry of Organic Compounds*, Wiley, New York, **1994**.
- [9] M. Levitt, A. Warshel, *J. Am. Chem. Soc.* **1978**, *100*, 2607.
- [10] H. L. Strauss, *Annu. Rev. Phys. Chem.* **1983**, *34*, 301.
- [11] a) J. P. Simons, R. A. Jockusch, P. Çarçabal, I. Hünig, R. T. Kroemer, N. A. McLeod, L. C. Snoek, *Int. Rev. Phys. Chem.* **2005**, *24*, 489; b) J. Screen, E. C. Stanca-Kaposta, D. P. Gamblin, B. Liu, N. A. McLeod, L. C. Snoek, B. G. Davis, J. P. Simons, *Angew. Chem.* **2007**, *119*, 3718; *Angew. Chem. Int. Ed.* **2007**, *46*, 3644; c) E. J. Cocinero, D. P. Gamblin, B. G. Davis, J. P. Simons, *J. Am. Chem. Soc.* **2009**, *131*, 11117; d) E. J. Cocinero, E. C. Stanca-Kaposta, M. Dethlefsen, B. Liu, D. P. Gamblin, B. G. Davis, J. P. Simons, *Chem. Eur. J.* **2009**, *15*, 13427; e) E. C. Stanca-Kaposta, D. P. Gamblin, E. J. Cocinero, J. Frey, R. T. Kroemer, A. J. Fairbanks, B. G. Davis, J. P. Simons, *J. Am. Chem. Soc.* **2008**, *130*, 10691.
- [12] a) F. O. Talbot, J. P. Simons, *Phys. Chem. Chem. Phys.* **2002**, *4*, 3562; b) R. A. Jockusch, F. O. Talbot, J. P. Simons, *Phys. Chem. Chem. Phys.* **2003**, *5*, 1502; c) P. Çarçabal, R. A. Jockusch, I. Hünig, L. C. Snoek, R. T. Kroemer, B. G. Davis, D. P. Gamblin, I. Compagnon, J. Oomens, J. P. Simons, *J. Am. Chem. Soc.* **2005**, *127*, 11414; d) I. Hünig, A. J. Painter, R. A. Jockusch, P. Çarçabal, E. M. Marzluff, L. C. Snoek, D. P. Gamblin, B. G. Davis, J. P. Simons, *Phys. Chem. Chem. Phys.* **2005**, *7*, 2474.
- [13] a) E. J. Cocinero, P. Çarçabal, T. D. Vaden, J. P. Simons, B. G. Davis, *Nature* **2011**, *469*, 76; b) E. J. Cocinero, P. Çarçabal, T. D. Vaden, J. P. Simons, B. G. Davis, *J. Am. Chem. Soc.* **2011**, *133*, 4548.
- [14] J.-P. Schermann, *Spectroscopy and Modelling of Biomolecular Building Blocks*, Elsevier, Amsterdam, **2008**.
- [15] a) J. U. Grabow, W. Caminati in *Frontiers of Molecular Spectroscopy* (Ed.: J. Laane), Elsevier, Amsterdam, **2009**, chap. 14; b) W. Caminati, J. U. Grabow in *Frontiers of Molecular Spectroscopy* (Ed.: J. Laane), Elsevier, Amsterdam, **2009**, chap. 15.

- [16] R. A. Motiyenko, E. A. Alekseev, S. F. Dyubko, F. J. Lovas, *J. Mol. Spectrosc.* **2006**, *240*, 93.
- [17] R. Larralde, M. P. Robertson, S. L. Miller, *Proc. Natl. Acad. Sci. USA* **1995**, *92*, 8158.
- [18] J. Fritzsche, Diplomarbeit, Gottfried-Wilhelm-Leibniz Universität Hannover, **2006**.
- [19] The decomposition products identified included glycoaldehyde, glyceraldehyde, hydroxypropanal, malonaldehyde, dihydroxyacetone, formaldehyde, and propinal.
- [20] E. J. Cocinero, A. Lesarri, P. Écija, J.-U. Grabow, J. A. Fernández, F. Castaño, *Phys. Chem. Chem. Phys.* **2010**, *12*, 12486.
- [21] a) A. Lesarri, S. Mata, E. J. Cocinero, S. Blanco, J. C. López, J. L. Alonso, *Angew. Chem.* **2002**, *114*, 4867; *Angew. Chem. Int. Ed.* **2002**, *41*, 4673; b) A. Lesarri, S. Mata, J. C. López, J. L. Alonso, *Rev. Sci. Instrum.* **2003**, *74*, 4799; c) J. L. Alonso, E. J. Cocinero, A. Lesarri, M. E. Sanz, J. C. López, *Angew. Chem.* **2006**, *118*, 3551; *Angew. Chem. Int. Ed.* **2006**, *45*, 3471.
- [22] a) A. Lesarri, R. Sánchez, E. J. Cocinero, J. C. López, J. L. Alonso, *J. Am. Chem. Soc.* **2005**, *127*, 12952; b) E. J. Cocinero, A. Lesarri, J.-U. Grabow, J. C. López, J. L. Alonso, *ChemPhysChem* **2007**, *8*, 599.
- [23] a) D. Banser, M. Schnell, J.-U. Grabow, E. J. Cocinero, A. Lesarri, J. L. Alonso, *Angew. Chem.* **2005**, *117*, 6469; *Angew. Chem. Int. Ed.* **2005**, *44*, 6311; b) A. Lesarri, R. D. Suenram, R. D. Brugh, *J. Chem. Phys.* **2002**, *117*, 9651.
- [24] T. A. Halgren, *J. Comput. Chem.* **1999**, *20*, 738.
- [25] Y. Zhao, D. G. Truhlar, *Acc. Chem. Res.* **2008**, *41*, 157.
- [26] W. Gordy, R. L. Cook, *Microwave Molecular Spectra*, Wiley, New York, **1984**.
- [27] J. K. Watson in *Vibrational Spectra and Structure*, Vol. 6 (Ed.: J. R. Durig), Elsevier, Amsterdam, **1977**, pp. 1–89.
- [28] G. T. Fraser, R. D. Suenram, C. L. Lugez, *J. Phys. Chem. A* **2000**, *104*, 1141.
- [29] R. S. Ruoff, T. D. Klots, T. Emilsson, H. S. Gutowsky, *J. Chem. Phys.* **1990**, *93*, 3142.
- [30] M. N. R. Ashfold, F. Claeysens, G. M. Fuge, S. J. Henley, *Chem. Soc. Rev.* **2004**, *33*, 23.
- [31] a) P. Deslongchamps, *Stereoelectronic Effects in Organic Chemistry*, Pergamon, New York, **1983**; b) G. R. J. Thatcher, *The Anomeric Effect and Associated Stereoelectronic Effects*, American Chemical Society, Washington, DC, **1993**.
- [32] a) T. J. Balle, W. H. Flygare, *Rev. Sci. Instrum.* **1981**, *52*, 33; b) J.-U. Grabow, W. Stahl, *Z. Naturforsch. A* **1990**, *45*, 1043; c) J.-U. Grabow, W. Stahl, H. Dreizler, *Rev. Sci. Instrum.* **1996**, *67*, 4072.
- [33] D. E. Powers, S. G. Hansen, M. E. Geusic, A. C. Pulu, J. B. Hopkins, T. G. Dietz, M. A. Duncan, P. R. R. Langridge-Smith, R. E. Smalley, *J. Phys. Chem.* **1982**, *86*, 2556.
- [34] R. D. Suenram, F. J. Lovas, G. T. Fraser, K. Matsumura, *J. Chem. Phys.* **1990**, *92*, 4724.
- [35] K. A. Walker, M. C. L. Gerry, *J. Mol. Spectrosc.* **1997**, *182*, 178.
- [36] Gaussian09, M. J. Frisch et al., Gaussian Inc., Wallingford CT, **2010**.